Kinetics and Thermodynamics of Calcium-Induced Lateral Phase Separations in Phosphatidic Acid Containing Bilayers†

Ian Graham, Jeannine Gagné, and John R. Silvius*
Department of Biochemistry, McGill University, Montréal, Québec, Canada H3G 1Y6
Received April 30, 1985

ABSTRACT: The effects of calcium on the mixing of synthetic diacylphosphatidylcholines (PC's) and diacylphosphatidylethanolamines (PE's) with the corresponding phosphatidic acids (PA's) have been examined by high-sensitivity differential scanning calorimetry and by measurements of the fluorescence of labeled PA or PC species in PA–PC bilayers. Calorimetrically derived phase diagrams for dimyristoyl- and dielaidoyl-substituted PA–PC and PA–PE mixtures indicate that these species are readily miscible in the absence of calcium but phase-separate very extensively in the presence of high levels of calcium (30 mM). The limiting solubilities of PA (Ca^{2+}) in liquid-crystalline PC or PE bilayers are $\leq$10 and $\sim$5 mol %, respectively, while $\sim$20 mol % of PC or PE can be introduced into the "cochleate" phase of PA (Ca^{2+}) before a distinct PC-rich (or PE-rich) phase appears. The kinetics of calcium-induced lateral phase separations were examined for dioleoyl- and dielaidoyl-substituted PA–PC unilamellar vesicles labeled with fluorescent (C_{12}-NBD-acyl) PA or PC, whose fluorescence becomes partially quenched upon phase separation. Our results indicate that, for the PA–PC system, lateral phase separation is very rapid ($\lesssim$1 s) after calcium addition and develops partially (possibly in only one face of the bilayer) when calcium is present only on one side of the bilayer. Moreover, phase separations can develop at a rate faster than that of vesicle diffusion when calcium is added to dilute suspensions of vesicles, suggesting that interbilayer contacts are not essential to promote phase separations.

Model membranes containing phosphatidic acid (PA)[1] have been used in numerous studies in recent years to examine the behavior of anionic lipids in membranes and the modulation of this behavior by multivalent cations. The addition of divalent cations to vesicles containing various species of PA can induce vesicle fusion (Papahadjopoulos et al., 1976; Koter et al., 1978; Liao & Prestegard, 1977; Sundler & Papahadjopoulos, 1981), phase separations (Ohnishi & Ito, 1974; Galla & Sackmann, 1975; Jacobson & Papahadjopoulos, 1975; Hartmann et al., 1977; Van Dijck et al., 1978), liquid-crystalline to solid lamellar phase transitions (Liao & Prestegard, 1981), or even lamellar to nonlamellar phase transitions (Papahadjopoulos et al., 1976; Verkleij et al., 1982; Farren et al., 1983) under appropriate experimental conditions. These phenomena provide useful models for similar processes mediated by other anionic lipids that are more abundant in natural membranes, such as phosphatidylserine and cardiolipin (Rand & Sengupta, 1972; Papahadjopoulos et al., 1977; Cullis et al., 1978; Wilschut et al., 1982; Verkleij, 1984). The very simple head-group structure of PA offers particular advantages in defining and modeling in detail the nature of the interactions between cations and a negatively charged lipid. Also, the production of PA from other phospholipids by phospholipase D digestion offers one of the few methods available whereby the phospholipid head-group composition of a lipid bilayer can be easily modified in situ without producing lipid species not found in natural membranes (de Kruijff & Baken, 1978; Clancy et al., 1981; Philipson & Nishimoto, 1984). Therefore, while PA is normally a minority species in natural membranes, model systems containing this lipid offer substantial advantages for studying the behavior of anionic lipids in membranes.

Previous studies using electron spin resonance (Ohnishi & Ito, 1974; Galla & Sackmann, 1975), freeze-fracture electron microscopy (Hartmann et al., 1977; Van Dijck et al., 1978; Verkleij et al., 1982), differential scanning calorimetry (Jacobson & Paphadjopoulos, 1975; Van Dijck et al., 1978), and X-ray diffraction (Caffrey & Feigenson, 1984) have provided evidence that dispersions of PA and PC exhibit lateral phase separations in the presence of calcium. However, few of these studies have examined the behavior of a PA–PC system that is a true binary lipid mixture amenable to a rigorous thermodynamic description, and no comparable studies of PA–PE mixtures have been reported to date. In this study, we have used high-sensitivity differential scanning calorimetry to characterize the mixing behavior of several PA–PC and PA–PE mixtures of homogeneous fatty acyl composition in the presence and absence of calcium ions. These measurements have been combined with studies of the behavior of fluorescent lipid probes in PA–PC vesicles in order to characterize both the kinetics and the extent of calcium-induced lateral phase separations in lipid bilayers containing PA together with neutral phospholipids. The following paper (Kouaouci et al., 1985) presents the results of a parallel Raman spectroscopic study of the DMPA–DMPC system before and after calci-

† This work was supported by grants from the Medical Research Council of Canada (ME-7580 and MA-7776) and the Fonds de la recherche en santé du Québec (820040). I.G. was the recipient of a National Science and Engineering Research Council (Canada) predoctoral fellowship award.

[1] Abbreviations: C_{12}-NBD-PA, 1-palmitoyl-2-[12-[(7-nitro-2,1,3-benzoxadiazol-4-yl)amino]dodecanoyl]-*sn*-glycerol 3-phosphate; C_{12}-NBD-PC, 1-palmitoyl-2-[12-[(7-nitro-2,1,3-benzoxadiazol-4-yl)amino]dodecanoyl]-*sn*-glycero-3-phosphocholine; DE, dielaidoyl; DM, dimyristoyl; DO, dioleoyl; DP, dipalmitoyl; DPePA, 1,2-dipentadecanoyl-*sn*-glycerol 3-phosphate; EDTA, ethylenediaminetetraacetic acid trisodium salt; egg PA, phosphatidic acid derived from egg lecithin; LUV, large unilamellar vesicle(s); PA, 1,2-diacyl-*sn*-glycerol 3-phosphate; PC, 1,2-diacyl-*sn*-glycero-3-phosphocholine; PE, 1,2-diacyl-*sn*-glycero-3-phosphoethanolamine; PS, 1,2-diacyl-*sn*-glycero-3-phosphoserine; Tes, *N*-[tris(hydroxymethyl)methyl]-2-aminoethanesulfonic acid; TLC, thin-layer chromatography.

0006-2960/85/0424-7123$01.50/0

um-induced phase separation, providing complementary information on the microscopic structures of the lipid phases that this and similar systems can adopt.

Materials and Methods

Materials

L-α-Glycero-3-phosphocholine–cadmium chloride adduct was obtained from Sigma (St. Louis, MO). 4-Pyrrolidinopyridine (98%) was purchased from Aldrich (Milwaukee, WI) and purified as described previously (Silvius & Gagné, 1984a). Phospholipase D from savoy cabbage was prepared as described elsewhere (Silvius & Gagné, 1984a). C_{12}-NBD-PC was obtained from Avanti Polar Lipids (Birmingham, AL). Ionophore A23187 was a product of Calbiochem (La Jolla, CA). All common inorganic chemicals were of at least reagent grade, and all solvents were freshly redistilled before use.

Methods

Synthesis of Phosphatidic Acids. Pure synthetic phosphatidylcholines, prepared as described previously (Silvius & Gagné, 1984a), were converted to the corresponding PA species by phospholipase D treatment as described by Papahadjopoulos & Miller (1967). The PA was purified by chromatography on silicic acid columns packed in 95:5:0.1 $CHCl_3$–methanol–concentrated NH_4OH, eluting with an ascending gradient of methanol in chloroform. Pure PA was obtained at 22–25% methanol. The PA was finally purified by barium acetate precipitation (Comfurius & Zwaal, 1977) and precipitation from chloroform with 10 volumes of cold acetone. The final product was "Folch"-washed, first with cold 0.1 N HCl as the aqueous component and then 3 times with 0.5 M NaCl plus 0.1 M EDTA, pH 7.4 (Papahadjopoulos & Miller, 1967), before storage as a chloroform solution under nitrogen at −70 °C. C_{12}-NBD-PA was prepared as described by Nichols & Pagano (1983) and then extensively Folch-washed as described above. Both NBD-labeled phospholipids gave single spots, both by fluorescence and phosphorus staining and by TLC in 65:35:2.5:2.5 $CHCl_3$–methanol–H_2O–concentrated NH_4OH and in 50:15:10:10:5 $CHCl_3$–acetone–methanol–acetic acid–H_2O.

Preparation of Calorimetric Samples. Samples containing ~5 μmol of lipid phosphorus (and, for samples to be treated with calcium, 0.4 mol % A23187) were lyophilized from benzene or cyclohexane and redispersed in buffer (0.85 mL) below the transition temperature (except in the case of DOPA) by syringe or by vortexing until a relatively homogeneous suspension was obtained. For samples to be incubated without calcium, the suspending buffer was 160 mM NaCl, 20 mM histidine, 20 mM Tes, and 1 mM EDTA, pH 7.4 (calcium-free buffer), while samples to be incubated with calcium were initially suspended in 70 mM NaCl, 20 mM histidine, and 20 mM Tes, pH 7.4. Calcium-free samples were then warmed above the transition temperature of the pure PA component with only gentle swirling of the sample. The samples were subsequently incubated under nitrogen according to the following schedules: for DMPC–DMPA, 10 min at 54 °C, 3 h at 20 °C, and ≥12 h at 4 °C; for DMPE–DMPA, 10 min at 58 °C, and then 4 h at 20 °C; for DPePA–DMPA, 5 min at 68 °C, 4 h at 30 °C, and 4 h at 20 °C; for DEPC–DEPA, 10 min at 45 °C, 3 h at 20 °C, and 24 h at 4 °C; for DEPE–DEPA, 10 min at 50 °C, 4 h at 20 °C, and 12 h at 10 °C. In all cases, samples were cooled from one preincubation temperature to the next in the above sequences at a rate of 0.25 °C/min. Samples to be incubated with calcium were vortexed above the transition temperature and them combined with $CaCl_2$ (as a 1 M aqueous solution) to give a final calcium concentration of 30 mM. The samples were then incubated essentially as described above for calcium-free samples. Samples were checked by TLC after incubation to ensure the absence of lipid breakdown products. Other conditions of calorimetric analysis were as described by Silvius & Gagné (1984a). Samples were run at a scan rate of 25 °C/h except where otherwise noted.

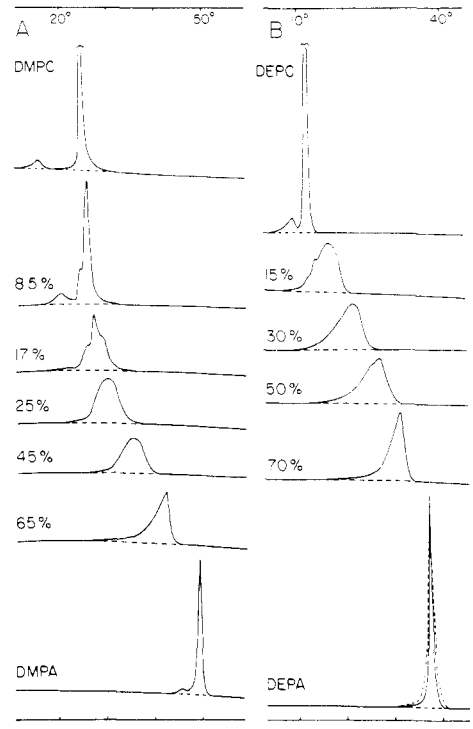

FIGURE 1: Thermograms recorded for (A) DMPA–DMPC and (B) DEPA–DEPC mixtures containing the indicated mole percent PA prepared in calcium-free buffer as described under Materials and Methods. In (B), the dashed curve represents the calorimetric thermogram obtained for a DEPA sample vortexed for 5 s at 45 °C, while the underlying solid curve was obtained with a DEPA dispersion treated identically but not vortexed above T_c.

Fluorescence Measurements. Large unilamellar lipid vesicles for fluorescence assays were prepared by reverse-phase evaporation followed by ultrafiltration through 0.1-μm pore size Nucleopore membranes (Wilschut et al., 1980). The fluorescence of NBD-labeled lipids was monitored by using the conditions described by Nichols & Pagano (1981). In all fluorescence experiments, the buffer used was 200 mM NaCl, 5 mM histidine, 5 mM Tes, and 0.1 mM EDTA, pH 7.4. Samples were prepared by diluting the vesicle stocks with this buffer and passing the diluted suspension 10 times through an 18-gauge syringe needle immediately before beginning each fluorescence measurement or time course. This step was found to be important to obtain reproducible results in experiments where the behavior of very dilute samples of vesicles was examined.

Results

Calorimetry of PA and PA–PC Mixtures. Representative thermograms obtained with samples of pure DEPA and DMPA in calcium-free buffer are shown in Figure 1. A small pretransition is seen just before the major endotherm in thermograms of DMPA samples run at scan rates ≤25 °C/h. When the temperature scan rate is decreased from 25 to 12 °C/h, the pretransition peak shifts to a temperature ~1 °C lower. Decreasing the sample pH from 7.4 to 6.0 shifts the DMPA pretransition from ~46 to ~30 °C. Curiously, the

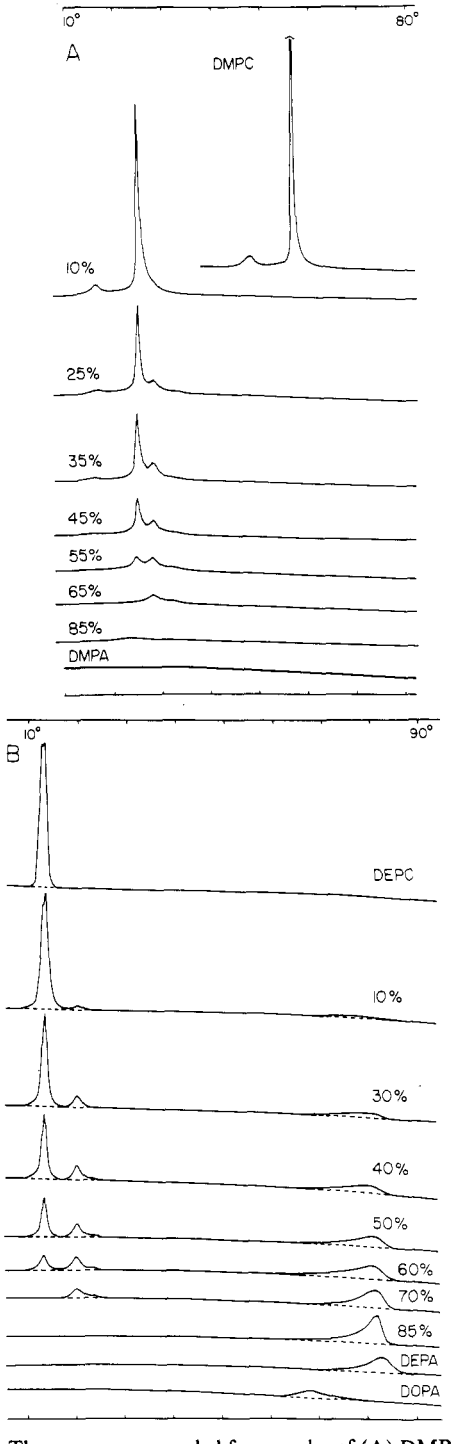

FIGURE 2: Thermograms recorded for samples of (A) DMPA–DMPC and (B) DEPA–DEPC (upper curves) or DOPA (lowest curve) prepared in the presence of calcium as described in the text. The molar percentage of PA contained in each sample is indicated above the corresponding trace.

thermograms of either DEPA or DMPA samples that are vortexed even briefly above their transition temperatures show main transition endotherms that are over twice as broad as those for nonvortexed samples, although their peak temperatures are unchanged (Figure 1B, dashed curve).

The addition of excess calcium to dispersions of pure DEPA and DMPA drastically perturbs the thermotropic behavior of these lipids, as shown in Figure 2. Pure DMPA (Ca^{2+}) forms an ordered cochleate phase (Liao & Prestegard, 1981) that exhibits no endothermic transitions from 5 to 95 °C, as reported previously (Van Dijck et al., 1978). However, DEPA (Ca^{2+}) exhibits a relatively broad endothermic transition

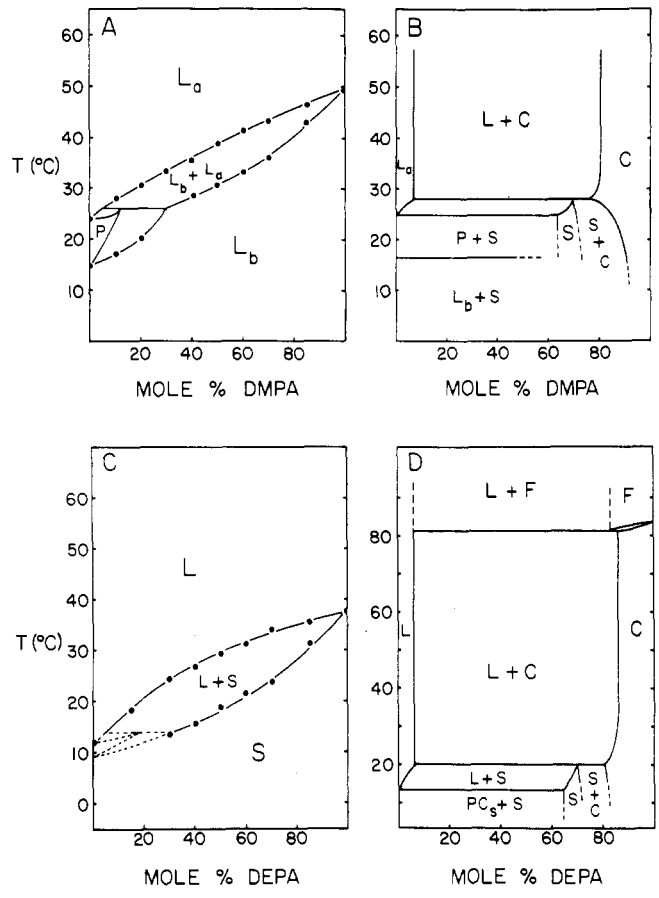

FIGURE 3: Phase diagrams determined for PA–PC mixtures by analysis of calorimetric results as described in the text. (A and B) DMPA–DMPC in the absence and presence of 30 mM $CaCl_2$, respectively; (C and D) DEPA–DEPC in the absence and presence of calcium, respectively. Phases are denoted as follows: L or L_a, hydrated liquid-crystalline lamellar; P and L_b, gel-state lamellar phases characteristic of pure DMPC above and below the pretransition; PC_s, gel-state lamellar phase of DEPC; S, solid solution; C, cochleate phase of PA–Ca^{2+}; F, fluid high-temperature phase of DEPA (Ca^{2+}).

centered at 83 °C, with an enthalpy of ~6 kcal mol^{-1}. DEPA (Ca^{2+}) samples prepared at pH 6.0 showed a broader transition at a slightly lower temperature. Samples of DOPA (Ca^{2+}) exhibit a similar broad endothermic transition, centered at 69 °C, when prepared at pH 7.4 or 7.1. However, dispersions of DOPA (Ca^{2+}) prepared at pH 6.8 or below showed no endothermic transitions from 5 °C up to at least 95 °C.

In Figure 1 are shown representative thermograms obtained with DMPA–DMPC and DEPA–DEPC mixtures in the absence of calcium. At low PA contents, the thermograms are somewhat complex in shape, as the pretransitions of the pure PC species are not wholly abolished by low mole fractions of PA. At higher PA contents, single broad endotherms are observed for both the dielaidoyl and the dimyristoyl lipid mixtures. Phase diagrams constructed from the calorimetric results are shown in panels A and C of Figure 3 for the DMPA–DMPC and DEPA–DEPC systems, respectively. In these phase diagrams and in those that follow, curves bounding regions of two-phase coexistence have been corrected to account for the finite transition widths for the pure individual components, using the procedure described by Mabrey & Sturtevant (1976).

Thermograms for DMPA–DMPC and DEPA–DEPC mixtures prepared in the presence of calcium are shown in Figure 2. For both systems, samples containing up to ~75 mol % PA exhibit sharp endotherms at the transition temperature of the pure PC component, suggesting that a phase

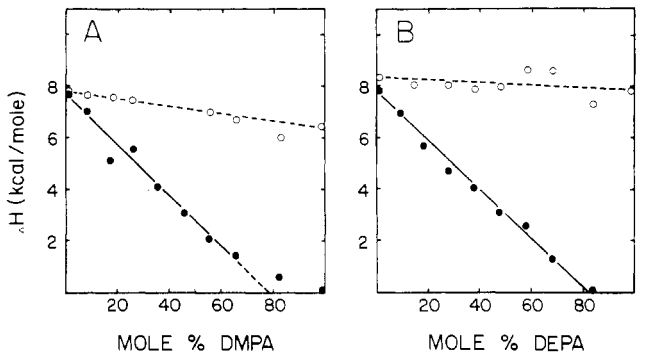

FIGURE 4: Integrated excess heat absorbed by (A) DMPA–DMPC and (B) DEPA–DEPC samples in the presence (closed circles) and absence (open circles) of calcium. For DEPA–DEPC (Ca^{2+}) samples, the enthalpy of the high-temperature transition has been neglected.

containing nearly pure PC is present in these samples at lower temperatures. From the thermograms recorded for various DMPA–DMPC (Ca^{2+}) and DEPA–DEPC (Ca^{2+}) mixtures, the phase diagrams for these binary lipid systems can be mapped, as outlined below for the DMPA–DMPC (Ca^{2+}) system.

As increasing amounts of DMPA (Ca^{2+}) are introduced into DMPC bilayers, sharp endotherms persist at the pretransition and main transition temperatures of pure DMPC up to PA levels of ~50 and ~65 mol %, respectively. These endotherms are mapped in the phase diagram of Figure 3B as horizontal lines representing the interconversions of phases containing nearly pure DMPC in equilibrium with a solid phase rich in DMPA (Ca^{2+}). A third endotherm is seen at a constant temperature of 28.1 °C in samples containing ≥5 and ≤75 mol % DMPA (Ca^{2+}). This calorimetric feature is mapped as a third line of three-phase coexistence on the phase diagram. To complete the phase diagram with the smallest possible number of distinct phases, we must postulate the existence of a solid solution containing relatively high levels of DMPA (Ca^{2+}), which decomposes at 28.1 °C to give a mixture of liquid-crystalline and cochleate lipid phases. The determination of the phase diagram shown in Figure 3B from the calorimetric data can then be completed in a straightforward manner, essentially as described previously for the PS–PE (Ca^{2+}) and PS–PC (Ca^{2+}) systems (Silvius & Gagné, 1984a,b).

The thermograms observed for DEPA–DEPC (Ca^{2+}) samples are qualitatively similar to those of DMPA–DMPC (Ca^{2+}) samples in most respects (Figure 2B). However, unlike DMPA (Ca^{2+}), DEPA (Ca^{2+}) shows an endothermic transition in the temperature range examined. This transition also appears, at a slightly lower but constant temperature, in samples containing from 85 down to ~10 mol % DEPA (Ca^{2+}), although the amplitude of this transition declines steadily with decreasing DEPA content. As the shape and position of the high-temperature transition endotherm are invariant in samples containing ~10–85% DEPA (Ca^{2+}), we have plotted this endotherm as an additional horizontal line in the phase diagram of Figure 3D. It is not clear whether the high-temperature phase of DEPA (Ca^{2+}) is lamellar or nonlamellar. Therefore, this phase, which coexists with a liquid-crystalline PC-rich phase at higher temperatures, is designated simply as F (for "fluid") in the phase diagram.

In Figure 4, the total excess heat absorbed by DMPA–DMPC and DEPA–DEPC samples, expressed per mole of phospholipid, is plotted vs. the mole fraction of PA in the samples. For samples prepared in the absence of calcium, the total excess heat absorption varies linearly with the mole

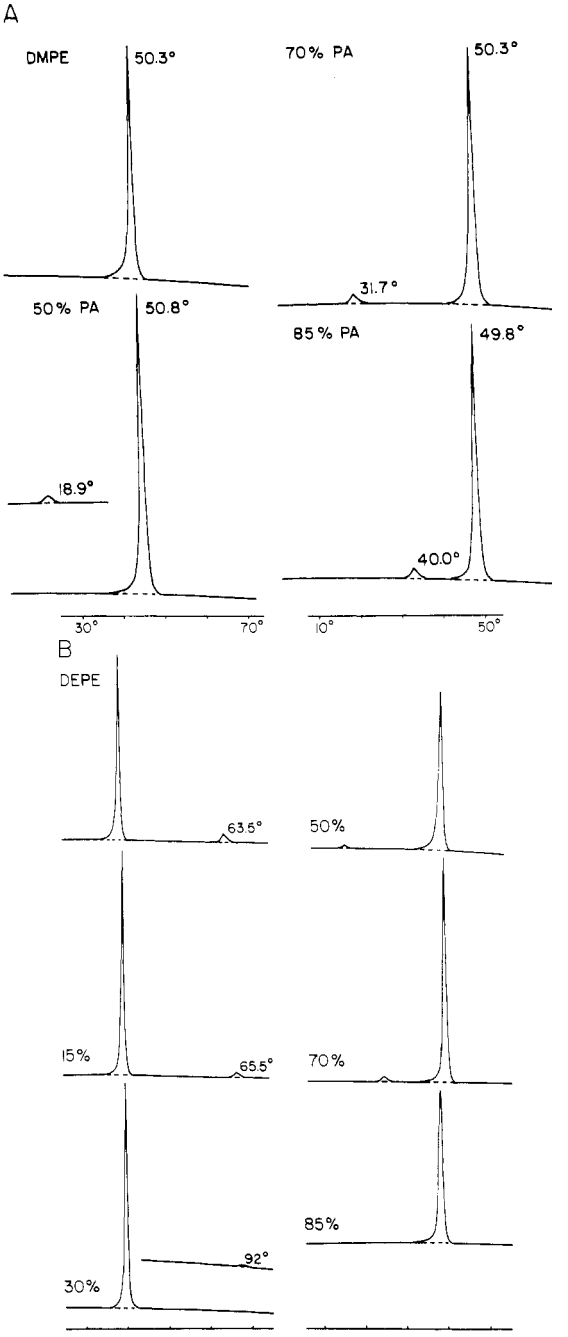

FIGURE 5: Thermograms recorded for (A) DMPA–DMPE and (B) DEPA–DEPE samples containing the indicated mole percent PA in calcium-free buffer. Details of sample preparation are given under Materials and Methods.

fraction of PA between the values measured for the pure PC and PA species. In the presence of calcium, the total excess heat absorbed by DMPA–DMPC samples over the experimental temperature range falls off almost linearly with increasing DMPA content, extrapolating to zero enthalpy at ~80–85% DMPA (Figure 4A). A similar result is obtained for DEPA–DEPC (Ca^{2+}) samples if the enthalpy of the high-temperature transition is neglected (Figure 4B). These results agree well with those predicted from the phase diagrams of Figure 3B,D if we assume that the conversion of lipid from gel or cochleate phases to the liquid-crystalline phase is strongly endothermic, while the transfer of lipid between the gel and cochleate phases is at most weakly so (Portis et al., 1979).

Calorimetry of PA–PE Mixtures. In Figure 5A are shown thermograms recorded for DMPA–DMPE mixtures in the

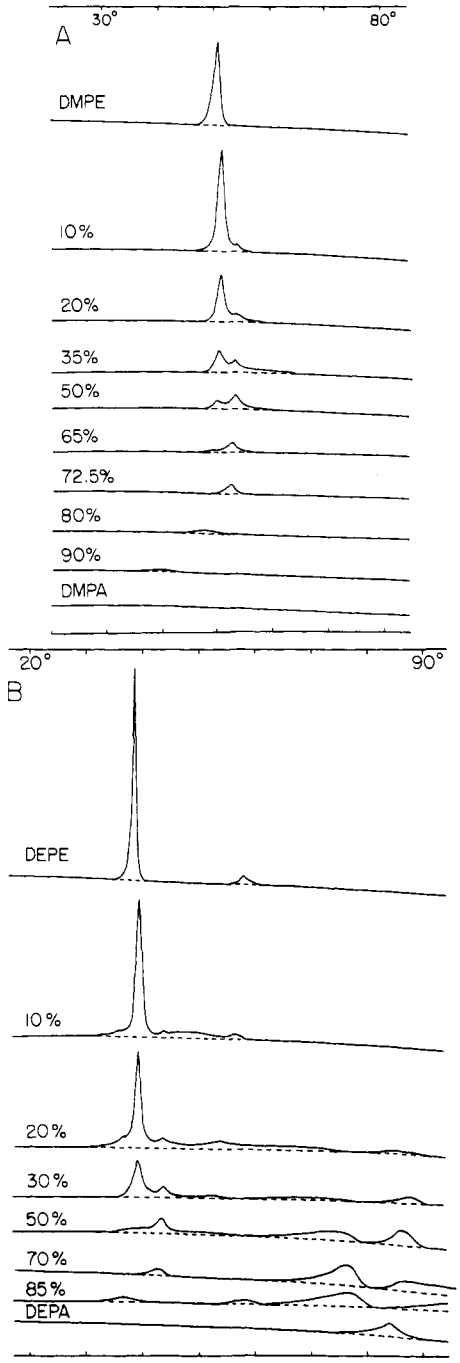

FIGURE 6: Thermograms recorded for (A) DMPA–DMPE and (B) DEPA–DEPE samples prepared in the presence of calcium. Samples containing the indicated mole percent PA were prepared as described in the text.

absence of divalent cations. The main transition endotherm remains sharp and almost constant in temperature for all proportions of DMPA and DMPE, as would be expected from the nearly identical transition temperatures of the pure lipid species. However, the small pretransition observed at 46 °C for pure DMPA shifts to progressively lower temperatures, without changing discernibly in sharpness or amplitude, as the proportion of DMPE increases from 0 to 50 mol %. Mixtures of DPePA with DMPE gave qualitatively similar thermograms (not shown). However, thin-layer chromatography showed slight decomposition of the PE component (≤5%) in DMPE–DPePA mixtures after preequilibration as described under Materials and Methods followed by calorimetric scanning to 70 °C. Calorimetrically derived phase diagrams for the DMPA–DMPE and DPePA–DMPE systems in the absence

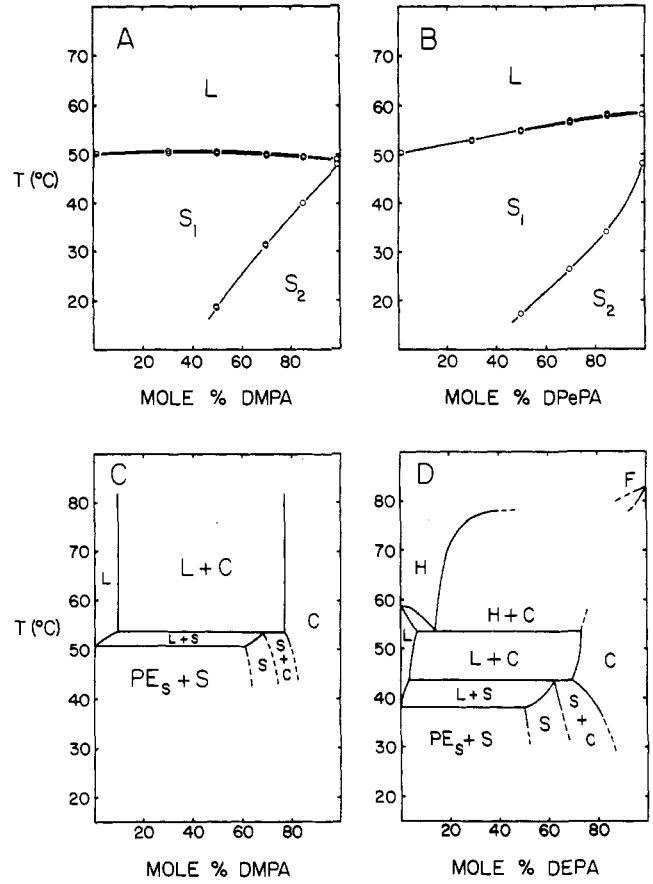

FIGURE 7: Phase diagrams derived from calorimetric data for (A) the DMPA–DMPE and (B) DPePA–DMPE systems in the absence of calcium, (C) the DMPA–DMPE system in the presence of calcium, and (D) the DEPA–DEPE system in the presence of calcium. Phases are denoted by the same symbols used in Figure 4 plus the symbol H for the hexagonal II phase of DEPE, S_1 and S_2 for distinct solid solutions of PE with PA, and PE_s for the gel-state lamellar phase of DEPE.

of calcium are plotted in panels A and B, respectively, of Figure 7.

For mixtures of DEPA and DEPE prepared in calcium-free buffer, the main transition endotherm again remains nearly unchanged in sharpness and peak temperature at various mole fractions of PA in PE (Figure 5B). However, the small endotherm observed at 63.5 °C for pure DEPE, which represents the lamellar to hexagonal II transition of this lipid, shifts to progressively higher temperatures as the bilayer PA content increases and can no longer be seen below 95 °C at 50 mol % DEPA. Interestingly, a small sharp lower temperature endotherm is seen in samples containing ~30–70 mol % DEPA.

The calorimetric behavior of DMPA–DMPE samples in the presence of excess calcium (Figure 6A) is in many respects similar to that of DMPA–DMPC (Ca^{2+}) samples (Figure 6A). The phase diagram for the DMPA–DMPE (Ca^{2+}) system (Figure 7C) is extracted from the calorimetric results by an analysis similar to that discussed above for the DMPA–DMPC (Ca^{2+}) system. Analysis of the experimental thermograms and of measured transition enthalpies (data not shown) for DMPA–DMPE (Ca^{2+}) mixtures indicates that the limiting solubility of DMPA (Ca^{2+}) in liquid-crystalline DMPE bilayers is ~5 mol %, while the cochleate phase of DMPA–Ca^{2+} can accommodate ~20 mol % DMPE at higher temperatures. The calorimetric behavior of DEPA–DEPE (Ca^{2+}) samples is considerably more complex, as shown in Figure 6B. The portions of the thermograms up to the small peak at 43.5 °C

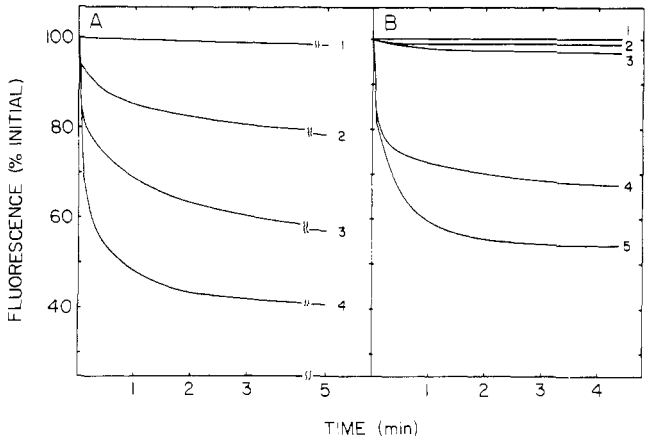

FIGURE 8: (A) Time course of fluorescence quenching after the addition of 10 mM calcium to LUV containing DEPA, DEPC, and NBD-PA in the following molar proportions: (1) 0:100:0.5, (2) 20:80:0.2, (3) 50:50:0.5, (4) 85:15:0.85. (B) Time courses of calcium-induced fluorescence quenching for LUV containing DOPA, DOPC, and NBD-PA in molar proportions of 50:50:0.5 (curve 1), 85:15:0.5 (curve 3), or 45:50:5 (curve 4), or DOPA, DOPC, and NBD-PC in molar proportions of 50:50:0.5 (curve 2) or 50:45:5 (curve 5). Experimental details are given in the text.

can be analyzed similarly to the thermograms obtained for DMPA–DMPE (Ca^{2+}) samples. Above this temperature, however, both DEPE and DEPA (Ca^{2+}) exhibit additional phase transitions in the pure state which must be included in the phase diagram for the DEPA–DEPE (Ca^{2+}) system. The lamellar to hexagonal II phase transition endotherm observed at 58 °C for pure DEPE in the presence of calcium diminishes in amplitude and shifts to slightly lower temperatures in mixtures containing up to ~50 mol % DEPA (Ca^{2+}), and small but finite excess heat absorption is observed above and/or below this peak in mixtures of widely varying DEPA (Ca^{2+}) content. The thermotropic behavior of DEPA–DEPE (Ca^{2+}) mixtures above ~70 °C is considerably more complex than that of DEPA–DEPC (Ca^{2+}) mixtures (Figure 2B). We therefore have not attempted to incorporate the high-temperature phases of DEPA (Ca^{2+}) into the partial phase diagram shown in Figure 7D.

Fluorescence Studies. The fluorescence of NBD-labeled phospholipids in a lipid bilayer is subject to significant self-quenching when the concentration of the fluorescent species in a particular region of the bilayer exceeds ~1 mol % (Nichols & Pagano, 1981). Accordingly, the fluorescence of an NBD-labeled lipid incorporated into lipid vesicles will reflect its distribution in the bilayer plane if its concentration is high enough for self-quenching effects to be significant (e.g., 5 mol %). We therefore examined the effects of calcium on the fluorescence of NBD-PA and -PC in large unilamellar vesicles containing PA and PC in order to investigate the kinetics of lipid redistribution during calcium-induced phase separations.

In the first series of experiments, we examined the effects of excess calcium (10 mM) on the fluorescence of NBD-PA and -PC in LUV containing DEPA and DEPC in various proportions. Except where specifically noted otherwise, the level of NBD-labeled species in these experiments was adjusted to be equal to 1% of the amount of the corresponding unlabeled species with the same head group. At this bulk concentration of the fluorescent lipid, self-quenching effects are minimal. Rather surprisingly, therefore, we found that calcium addition caused a large and rapid decrease in the fluorescence of NBD-PA in vesicles containing DEPA and DEPC in an 85:15 molar ratio, as shown in Figure 8A. When the level of NBD-PA in such vesicles was decreased from 0.85 to 0.10 mol %, the extent of fluorescence quenching induced by calcium was the same. As this fluorescence quenching is independent of the NBD-PA concentration at low levels of fluorophore, it is probably attributable not to probe–probe interactions but rather to a change in the environment of the NBD group upon addition of calcium. Comparable quenching was also observed when DEPA vesicles containing small amounts of NBD-PA were cooled below their transition temperature in the absence of calcium (not shown), suggesting that such quenching arises from the conversion of the DEPA to a state with highly ordered acyl chains. Calcium produced an almost equal quenching of the fluorescence of NBD-PA in vesicles containing DEPA and DEPC in a 50:50 molar ratio, and a somewhat smaller but still substantial quenching of NBD-PA fluorescence was seen upon calcium addition to 20:80 (mol/mol) DEPA–DEPC vesicles. These calcium-induced fluorescence changes could be rapidly reversed by adding a 2-fold excess of EDTA, which was pretitrated with base to neutralize excess protons released by the EDTA–Ca^{2+} interaction. No change in fluorescence was induced by calcium addition to vesicles containing 0.5 mol % NBD-PA in DEPC.

In contrast to the results obtained with NBD-PA, only a small fluorescence quenching (≥10%) was seen when calcium was added to 50:50 (mol/mol) DEPA–DEPC vesicles containing 0.5 mol % NBD-PC. Calcium caused no quenching of the fluorescence of NBD-PC incorporated to a level of 0.8 mol % in 20:80 (mol/mol) DEPA–DEPC vesicles or in vesicles containing only DEPC.

The results obtained with NBD-PA in DEPA–DEPC vesicles can be readily rationalized with reference to the DEPA–DEPC (Ca^{2+}) phase diagram of Figure 3D if we note that the fluorescence of NBD-PA becomes partially quenched, regardless of its concentration in the bilayer, when it is incorporated into gellike PA (Ca^{2+}) rich domains. The phase diagram of Figure 3D indicates that bilayers containing more than 5–10% DEPA will form such segregated domains at equilibrium. We thus expect that the fluorescence of NBD-PA, which should be concentrated in the PA-rich domains, will decrease substantially after the addition of calcium to bilayers containing even relatively low amounts of DEPA (e.g., 20 mol %). This prediction agrees well with the experimental results presented above. It is also readily understandable that calcium causes minimal changes in the fluorescence of low concentrations of NBD-PC in 50:50 or 20:80 (mol/mol) DEPA–DEPC vesicles, for NBD-PC should be preferentially associated with PC-rich domains, where its fluorescence will remain unquenched, after phase separation. It thus appears that measurements of the fluorescence of NBD-PA can be used to monitor the calcium-induced formation of PA-rich domains in DEPA–DEPC vesicles and that the kinetics of this process are rapid (approximately seconds to minutes).

A complementary method to monitor Ca^{2+}-induced phase separations in PA–PC bilayers is provided by the use of DOPA–DOPC vesicles containing relatively high concentrations of NBD-PA or -PC. As shown in Figure 8B, the addition of calcium to vesicles containing DOPA, DOPC, and NBD-PA in an 85:15:1 molar ratio causes only a small decrease in fluorescence. Similarly, calcium addition causes only small changes in the fluorescence of vesicles containing equimolar proportions of DOPA and DOPC plus 0.5 mol % NBD-PA or NBD-PC. However, the addition of calcium causes large decreases in the fluorescence of vesicles containing DOPA, DOPC, and NBD-PC in a 50:45:5 molar ratio, or DOPA, DOPC, and NBD-PA in a 45:50:5 molar ratio. The fluorescence changes induced by calcium in these lipid mixtures

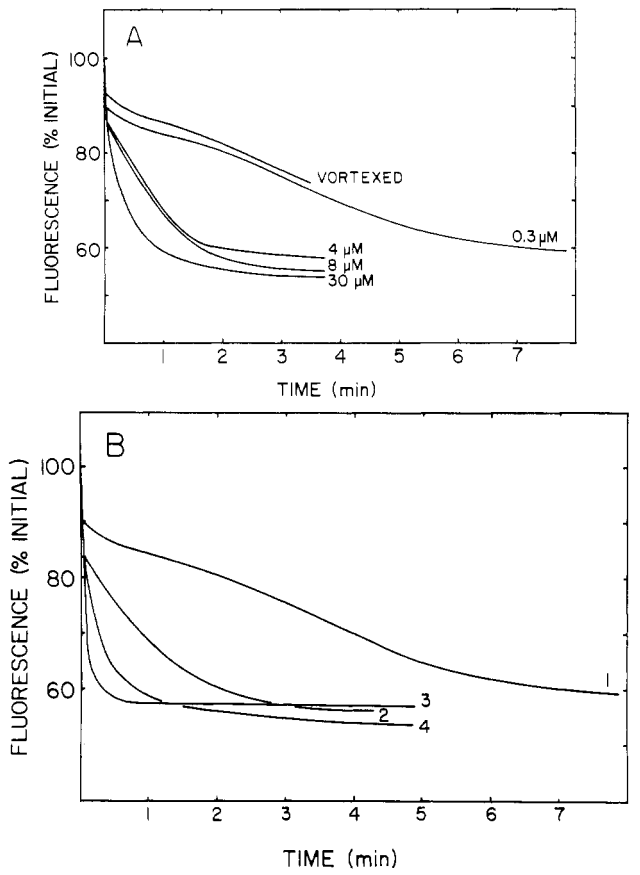

FIGURE 9: (A) Fluorescence of vesicles composed of 50:45:5 DOPA–DOPC–NBD-PC after addition of calcium (10 mM). Top curve, vesicles prepared by very gentle dispersal of a dried lipid film; lower curves, ~1000-Å LUV at the indicated total lipid concentrations. (B) Fluorescence time courses after addition of 10 mM $CaCl_2$ to 50:45:5 DOPA–DOPC–NBD-PC LUV with or without ionophore A23187. Curve 1, 0.3 μM lipid, no ionophore; curve 2, 0.3 μM lipid, 1:200 moles of A23187/mole of lipid; curve 3, 0.3 μM lipid, 1:50 moles of A23187/mole of lipid; (4) 40 μM lipid, no ionophore. Experimental details are as for Figure 8.

can again be readily reversed by addition of a 2-fold excess of EDTA. These results indicate that the fluorescence of NBD-PA or -PC in DOPA–DOPC bilayers is sensitive to calcium when the concentration of fluorescent lipid is high enough for self-quenching of fluorescence to be significant, but not when the fluorophore concentration is much lower. It thus appears that calcium can influence the fluorescence of NBD-PC or -PA in DOPA–DOPC vesicles only by causing lateral redistribution of the lipids and not simply by causing a change in the physical state of the bilayer, in contrast to the results obtained with the DEPA–DEPC–NBD-PA system. This finding is quite important, as it indicates that fluorescence changes induced by calcium in DOPA–DOPC vesicles containing either NBD-PA or NBD-PC can be attributed entirely to lateral redistribution of lipids in the bilayer.

The fluorescence experiments discussed to this point were all carried out with phospholipid vesicles at a relatively high lipid concentration (40 μM). The kinetics of calcium-induced fluorescence changes were also examined at lower lipid concentrations for vesicles of various types and compositions. The fluorescence traces shown in Figure 9A illustrate the effects of decreasing lipid concentration on the kinetics of the calcium-induced fluorescence decrease for LUV containing DOPA, DOPC, and NBD-PC in a 50:45:5 molar ratio. The time course of the fluorescence quenching after calcium addition to these vesicles has two components, one of which is at least as fast as the mixing time (1–2 s) while the other is

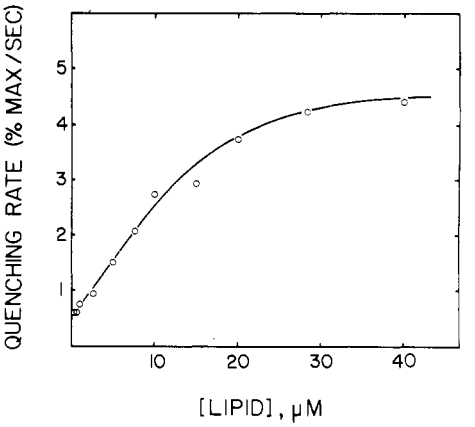

FIGURE 10: Rate of the slow phase of fluorescence quenching upon addition of calcium (10 mM) to 50:45:5 DOPA–DOPC–NBD-PC vesicles at various concentrations of total vesicle lipids. The rate of the slow phase of quenching is expressed as a percentage of the total slow phase amplitude per unit time.

considerably slower. As the vesicle concentration is gradually decreased, the fast component remains essentially unchanged, while the rate but not the amplitude of the slow component progressively decreases. The amplitude of the fast component of the fluorescence decrease is consistently comparable to but slightly less than that of the slow component. When the calcium ionophore A23187 is added to dilute suspensions of vesicles at nominal ionophore:lipid ratios of 1:50 or 1:200, the rate but not the amplitude of the slow phase of the fluorescence decrease is greatly enhanced (Figure 9B). The effect of the ionophore is much less at high lipid concentrations, where the "slow" phase of fluorescence quenching is already relatively rapid. Very similar results were obtained with LUV containing DOPA, DOPC, and NBD-PA in a 45:50:5 molar ratio or DEPA, DEPC, and NBD-PA in a 50:50:0.5 molar ratio (not shown).

When vesicles containing DOPA, DOPC, and NBD-PC in a 50:45:5 molar ratio are prepared by gently vortexing a dried lipid film with buffer, the addition of calcium again causes a biphasic decrease in fluorescence (Figure 9A). The fast component of the fluorescence drop in this case is slightly smaller than for LUV of the same composition, although the total decrease in fluorescence remains essentially the same as for the LUV. When the vortexed lipid dispersion was bath-sonicated for 30 s prior to calcium addition, the amplitude of the fast component of fluorescence quenching became comparable to or slightly greater than that for LUV (not shown). The incorporation of ionophore A23187 into vortexed lipid dispersions again increased the rate of the slow phase of fluorescence quenching without affecting the amplitude of either the fast or the slow phase.

The results presented above indicate that the slow component of fluorescence quenching observed after adding calcium to PA–PC vesicles can be accelerated either by adding a calcium ionophore to the vesicles or by increasing the concentration of vesicles. The effect of increasing vesicle concentration on the rate of the slow component is analyzed more quantitatively for 50:45:5 (molar ratio) DOPA–DOPC–NBD-PC vesicles in Figure 10. Here the initial rate of the slow component, expressed as a percentage decrease in fluorescence per unit time, is plotted as a function of the lipid concentration. At low concentrations of lipid, the plot is linear, indicating that the rate of the slow component rises as the second power of the vesicle concentration. This result suggests that vesicle–vesicle interactions promote the processes underlying the slow phase of fluorescence quenching. However,

the plot of Figure 10 extrapolates to a nonzero y intercept, indicating that the slow component of fluorescence quenching can develop, albeit at a low rate, even for an isolated vesicle. At high concentrations of vesicle lipid, the plot of Figure 10 begins to plateau, suggesting that the rate or extent of vesicle–vesicle interactions no longer limits the rate of the slow component at high lipid concentrations. Results similar to those shown in Figure 10 were also obtained using LUV containing DOPA, DOPC, and NBD-PA in a 45:50:5 molar ratio or DEPA, DEPC, and NBD-PA in a 50:50:0.5 molar ratio (not shown).

Discussion

The phase diagrams derived from our calorimetric results for the DEPA–DEPC and DMPA–DMPC systems indicate that these lipid pairs form binary solutions with good but not ideal miscibilty of the lipid components in the absence of divalent cations. The mixing of PA and PE species of the same acyl composition may be closer to ideal, as both the main transitions and, more surprisingly, the pretransitions observed for PA–PE samples appear to be as sharp as the corresponding transitions for the pure PA species. In agreement with the results of previous studies using electron spin resonance (Ohnishi & Ito, 1974; Galla & Sackmann, 1975) , X-ray diffraction (Caffrey & Feigenson, 1984), and freeze–fracture electron microscopy and scanning calorimetry (Jacobson & Papahadjopoulos, 1975; Hartmann et al., 1977; Van Dijck et al., 1978; Verkleij et al., 1982), our calorimetric results indicate that the addition of calcium to PA–PC mixtures induces extensive phase separation. However, our phase diagrams for the DEPA–DEPC (Ca^{2+}) and DMPA–DMPC (Ca^{2+}) systems indicate that the PA and PC components are not totally laterally segregated in the presence of calcium. While only a few mole percent of PA (Ca^{2+}) can be accommodated in a PC-rich liquid-crystalline phase, a significant amount of PC ($\sim$20 mol %) can be incorporated into bilayers rich in PA (Ca^{2+}) before a distinct PC-rich phase appears. These conclusions agree well with the results of Raman spectroscopic studies of the DMPA–DMPC (Ca^{2+}) system, which are presented in the following paper (Kouaouci et al., 1985). The phase separation induced by calcium in PA–PE bilayers is similar in extent to that observed in PA–PC bilayers. PE thus appears to mix more nearly ideally than does PC with PA and PS species of the same acyl composition in the absence of divalent cations [this study and Silvius & Gagné (1984a,b)]. In the presence of calcium, however, PE is no more miscible with these anionic lipids (and in some cases, less so) than is PC.

The structural basis of the high-temperature endothermic transitions observed for DOPA (Ca^{2+}) and DEPA (Ca^{2+}) samples cannot be entirely defined from the results obtained in this study. From the substantial heat contents of these transitions, we may assume that both unsaturated PA species form an ordered lamellar phase in the presence of calcium below the temperature of the broad endothermic transition. Farren et al. (1983) have reported that at 25 °C, DOPA (Ca^{2+}) forms hexagonal II structures at pH 6.0 but lamellar structures at pH 7.4. It could plausibly be suggested that as the sample pH is increased, the temperature of a lamellar to hexagonal II transition of DOPA (Ca^{2+}) gradually shifts upward, so that the 69 °C calorimetric transition seen at pH 7.4 represents a lamellar to hexagonal transition. However, our calorimetric results for DOPA (Ca^{2+}) samples prepared at pH values intermediate between 6.0 and 7.4 do not clearly support this suggestion. We consider it equally possible that at pH 7.4, DOPA (Ca^{2+}) and DEPA (Ca^{2+}) samples may form a liquid-crystalline lamellar phase at high temperatures that is distinct from the liquid-crystalline phase formed by neutral phospholipids. Caffrey & Feigenson (1984) have in fact reported that egg PA in the presence of cadmium chloride can form a liquid-crystalline lamellar phase that is immiscible with the liquid-crystalline phase of egg PC.

The kinetics of calcium-induced phase separations in PA–PC mixtures have not previously been investigated in detail. Ohnishi & Ito (1974) have reported that calcium addition induces rapid changes in the ESR spectrum of a spin-labeled PA incorporated into a PA–PC mixture deposited on Millipore filters. However, the precise time scale of the calcium-induced ESR spectral changes was not specified by these authors, although it can be inferred that times not longer than a few minutes are required. Moreover, it is difficult to extrapolate from results obtained with the system studied by these authors to predict the behavior of dilute dispersions of PA–PC vesicles. The results of our fluorescence experiments indicate that calcium can induce extensive lateral phase separations in large unilamellar PA–PC vesicles on a time scale of no longer than seconds. This time scale is much shorter than that reported by Hoekstra (1982) to be required for the lateral redistribution of N-NBD-PE in PC–PS bilayers after exposure to calcium (minutes to hours). However, as we have noted elsewhere (Silvius & Gagné, 1984b), it is not clear how the distribution of N-NBD-PE, an anionic species with a bulky head group, will respond to changes in the distribution of the majority lipid species in PC–PS mixtures upon addition of calcium. Preliminary results obtained with C_{12}-NBD-PC in DOPS–DOPC mixtures suggest that the limited phase separations that are induced by calcium in PS–PC bilayers do in fact exhibit kinetics comparable to those of phase separation in PA–PC mixtures (J. Silvius, unpublished results).

The results of our studies of the kinetics of phase separation after calcium addition to PA–PC vesicles indicate that the phase separation proceeds in two stages. The first stage of phase separation is very rapid ($\leq$1–2 s) and is unaffected by vesicle–vesicle contacts but is somewhat smaller for vesicles prepared by vortexing dried PA–PC films in buffer than for LUV prepared by reverse-phase evaporation. The second stage of phase separation is considerably slower than the first but is strongly promoted by vesicle–vesicle interactions or by the addition of small amounts of a calcium ionophore. Taken together, these findings strongly suggest that the first stage of calcium-induced phase separation occurs when calcium interacts with the outer surface of the vesicles and that the second stage occurs only after calcium has penetrated to the interior of the vesicles. Some additional implications of our fluorescence results are discussed below.

One of the most significant conclusions derived from our fluorescence studies of phase separation is that, at least for PA–PC vesicles, the induction of phase separation by calcium does not appear to require bilayer–bilayer contacts. Very dilute suspensions of vesicles ($\sim$0.3 μM lipid) treated with ionophore A23187 exhibit calcium-induced fluorescence changes that develop more rapidly than the theoretical rate of vesicle–vesicle collisions [calculated as in Lansman & Haynes (1975)] and are essentially as large (when expressed as a fraction of initial fluorescence) as those observed for much more concentrated suspensions of vesicles. It remains to be seen whether this behavior is also characteristic of lipid mixtures containing anionic lipids other than PA, which has a very high affinity for calcium. We are presently testing this point with bilayers containing PS, whose calcium-binding affinity is reported to be modified by intermembrane contacts (Ekerdt & Papa-

hadjopoulos, 1982). Our present findings suggest that for PA–PC vesicles, intermembrane contracts enhance the rate of calcium-induced lipid phase separations simply by facilitating calcium entry into the interior of the vesicles. We have in fact observed that the rate of calcium-induced leakage of carboxyfluorescein from PA–PC vesicles is strongly dependent on the vesicle concentration (J. Gagné and J. R. Silvius, unpublished results). Therefore, sites of intervesicular contact may represent points at which the vesicle permeability to low molecular weight solutes is nonspecifically increased at least transiently, and through which calcium may therefore enter the vesicles at an enhanced rate.

When PA–PC vesicles are exposed to calcium under conditions where calcium penetration into the vesicle interior is slow, fluorescence measurements indicate that a lateral redistribution of lipids occurs that is very rapid but that represents only part of the total lipid redistribution induced by calcium at equilibrium. It would be reasonable to suggest that this fast redistribution of lipids takes place only in the outer monolayer of the vesicle membrane. The results of Sillerud & Barnett (1981) add plausibility to this suggestion. These authors reported that bilayers of DMPC or DPPC, when asymmetrically perturbed by the addition of lanthanide ions to only one face of the bilayer, exhibit separate phase transitions in the two faces of the bilayer. Our experimental results suggest, although they do not prove, that lateral phase separations can likewise occur more or less independently at the two faces of an asymmetrically perturbed bilayer membrane.

The results of both our calorimetric and our fluorometric studies indicate that calcium induces extensive phase separations in PA–PC mixtures. Our fluorescence results indicate further that a lateral segregation of lipids occurs very rapidly (less than 1 s) after calcium addition to such mixtures. It cannot be assumed a priori that the very rapid lipid redistributions observed in our fluorescence studies represent the full time course of equilibration of PA–PC samples after calcium addition. However, the findings of Caffrey & Feigenson (1984) indicate that calcium induces the formation of a segregated and highly ordered cochleate phase in egg PA–egg PC bilayers within at most 10–30 min after its addition to vesicles containing these lipids. Van Dijck et al. (1978) have reported a similar result for DMPA–DMPC mixtures equilibrated for 10 min at 60 °C. The times of sample equilibration in these studies overlap the time scale examined in our fluorescence studies. We therefore believe that the rapid lipid redistributions that we detect fluorometrically upon calcium addition to liquid-crystalline PA–PC vesicles genuinely reflect the time course over which the lipid distribution in these vesicles approaches the equilibrium observed in our calorimetric studies and in the structural studies just cited.

ACKNOWLEDGMENTS

We thank Dr. Martin Zuckermann for valuable and stimulating discussions throughout the course of this work.

Registry No. DMPA, 28874-52-4; DMPC, 18194-24-6; DEPA, 98574-23-3; DEPC, 56782-46-8; DMPE, 998-07-2; DEPE, 19805-18-6; DPePA, 73731-64-3; DOPA, 61617-08-1; DOPC, 4235-95-4; Ca, 7440-70-2.

REFERENCES

Caffrey, M., & Feigenson, G. W. (1984) *Biochemistry 23*, 323.

Clancy, R. M., Wissenberg, A. R., & Glaser, M. (1981) *Biochemistry 20*, 6060.

Comfurius, P., & Zwaal, R. F. A. (1977) *Biochim. Biophys. Acta 488*, 36.

Cullis, P. R., Verkleij, A. J., & Ververgaert, P. H. J. T. (1978) *Biochim. Biophys. Acta 513*, 11.

de Krujff, B., & Baken, P. (1978) *Biochim. Biophys. Acta 507*, 38.

Ekerdt, R., & Papahadjopoulos, D. (1982) *Proc. Natl. Acad. Sci. U.S.A. 79*, 2273.

Farren, S. B., Hope, M. J., & Cullis, P. R. (1983) *Biochem. Biophys. Res. Commun. 111*, 2273.

Galla, H.-J., & Sackmann, E. (1975) *Biochim. Biophys. Acta 401*, 509.

Hartmann, W., Galla, H.-J., & Sackmann, E. (1977) *FEBS Lett. 78*, 169.

Hoekstra, D. (1982) *Biochemistry 21*, 2833.

Jacobson, K., & Papahadjopoulos, D. (1975) *Biochemistry 14*, 152.

Koter, M., de Kruijff, B., & van Deenen, L. L. M. (1978) *Biochim. Biophys. Acta 514*, 255.

Kouaouci, R., Silvius, J. R., Graham, I., & Pézolet, M. (1985) *Biochemistry* (following paper in this issue).

Lansmann, J., & Haynes, D. M. (1975) *Biochim. Biophys. Acta 394*, 335.

Liao, M.-J., & Prestegard, J. M. (1979) *Biochim. Biophys. Acta 550*, 1757.

Liao, M.-J., & Prestegard, J. M. (1981) *Biochim. Biophys. Acta 645*, 149.

Mabrey, S. J., & Sturtevant, J. N. (1976) *Proc. Natl. Acad. Sci. U.S.A. 73*, 3862.

Nichols, J. W., & Pagano, R. E. (1981) *Biochemistry 20*, 2783.

Nichols, J. W., & Pagano, R. E. (1983) *J. Biol. Chem. 258*, 5368.

Ohnishi, S., & Ito, T. (1974) *Biochim. Biophys. Acta 352*, 29.

Papahadjopoulos, D., & Miller, N. (1967) *Biochim. Biophys. Acta 135*, 624.

Papahadjopoulos, D., Vail, W. J., Pangborn, W. A., & Poste, G. (1976) *Biochim. Biophys. Acta 448*, 265.

Papahadjopoulos, D., Vail, W. J., Newton, C., Nir, S., Jacobason, K., Poste, G., & Lazo, R. (1977) *Biochim. Biophys. Acta 465*, 579.

Philipson, K. D., & Nishimoto, A. Y. (1984) *J. Biol. Chem. 259*, 16.

Portis, A., Newton, C., Pangborn, W., & Papahadjopoulos, D. (1979) *Biochemistry 18*, 780.

Rand, R. P., & Sengupta, S. (1972) *Biochim. Biophys. Acta 255*, 484.

Sillerud, L. O., & Barnett, R. E. (1982) *Biochemistry 21*, 1756.

Silvius, J. R., & Gagné, J. (1984a) *Biochemistry 23*, 3232.

Silvius, J. R., & Gagné, J. (1984b) *Biochemistry 23*, 3241.

Sundler, R., & Papahadjopoulos, D. (1981) *Biochim. Biophys. Acta 649*, 743.

Van Dijck, P. W. M., de Kruijff, B., Verkleij, A. J., van Deenen, L. L. M., & de Gier, J. (1978) *Biochim. Biophys. Acta 512*, 84.

Verkleij, A. J. (1984) *Biochim. Biophys. Acta 779*, 43.

Verkleij, A. J., de Maagd, R., Leunissen-Bijvelt, J., & de Kruijff, B. (1982) *Biochim. Biophys. Acta 684*, 255.

Wilschut, J., Düzgünes, N., Fraley, R., & Papahadjopoulos, D. (1980) *Biochemistry 19*, 6011.

Wilschut, J., Holsappel, M., & Jansen, R. (1982) *Biochim. Biophys. Acta 690*, 297.